JACS
JOURNAL OF THE AMERICAN CHEMICAL SOCIETY
Article
pubs.acs.org/JACS

Clickable Protein Nanocapsules for Targeted Delivery of Recombinant p53 Protein

Muxun Zhao,[†] Yarong Liu,[‡] Renee S. Hsieh,[†] Nova Wang,[†] Wanyi Tai,[§] Kye-Il Joo,[‡] Pin Wang,[‡] Zhen Gu,[§] and Yi Tang*[,†]

[†]Department of Chemical and Biomolecular Engineering and Department of Chemistry and Biochemistry, University of California, Los Angeles, California 90095, United States

[‡]Mork Family Department of Chemical Engineering and Materials Science, University of Southern California, Los Angeles, California 90089, United States

[§]Joint Department of Biomedical Engineering, University of North Carolina at Chapel Hill and North Carolina State University, Raleigh, North Carolina 27695, United States

Supporting Information

ABSTRACT: Encapsulating anticancer protein therapeutics in nanocarriers is an attractive option to minimize active drug destruction, increase local accumulation at the disease site, and decrease side effects to other tissues. Tumor-specific ligands can further facilitate targeting the nanocarriers to tumor cells and reduce nonspecific cellular internalization. Rationally designed non-covalent protein nanocapsules incorporating copper-free "click chemistry" moieties, polyethylene glycol (PEG) units, redox-sensitive cross-linker, and tumor-specific targeting ligands were synthesized to selectively deliver intracellular protein therapeutics into tumor cells via receptor-mediated endocytosis. These nanocapsules can be conjugated to different targeting ligands of choice, such as anti-Her2 antibody single-chain variable fragment (scFv) and luteinizing hormone releasing hormone (LHRH) peptide, resulting in specific and efficient accumulation within tumor cells overexpressing corresponding receptors. LHRH-conjugated nanocapsules selectively delivered recombinant human tumor suppressor protein p53 and its tumor-selective supervariant into targeted tumor cells, which led to reactivation of p53-mediated apoptosis. Our results validate a general approach for targeted protein delivery into tumor cells using cellular-responsive nanocarriers, opening up new opportunities for the development of intracellular protein-based anticancer treatment.

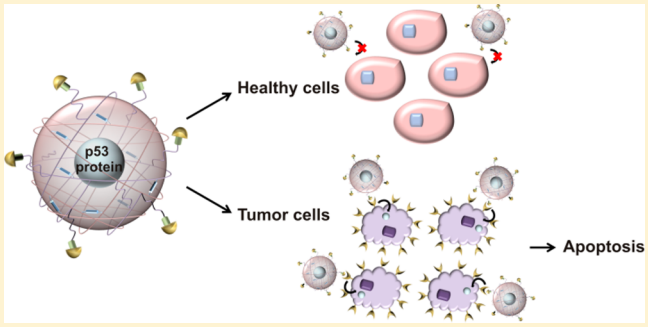

Virtually all human cancer cells have elaborate anti-apoptotic strategies to overcome apoptosis, which is a vital cellular mechanism to obstruct tumor progression.[1] The most commonly mutated gene in tumor cells is the tumor suppressor gene *TP53*, the protein product of which promotes apoptosis of aberrant cells through both transcription-dependent and -independent mechanisms.[2] In this manner, the genome guardian p53 is critically important in eliminating possible neoplastic cells incurred during DNA damage. About 50% of all human tumors have mutant p53 proteins.[3] Therefore, restoring p53 function can be a highly effective option for cancer treatment. Functional copies of p53 can not only resurrect the apoptotic circuitry but also sensitize the tumor cells toward other various treatments (radio- and chemotherapy).[4] Different strategies pursuing this goal have been intensively investigated, including small molecules and peptides that overcome p53 mutations as well as adenovirus/p53 gene delivery vectors.[5−8] While restoring p53 functions in cancer cells has been a tantalizing approach toward combating cancer, the lack of effective delivery methods has undermined its potential as an anticancer therapeutic.

Intracellular protein delivery using stimuli-responsive nanomaterials has emerged as an attractive method to deliver various cargos to cells of interest.[9−18] In particular, water-soluble polymer-based nanocarriers that encapsulate the protein of interest to aid penetration of the cellular membrane but are capable of releasing the protein upon various cellular stimuli have been demonstrated to be effective in functional delivery of proteins.[19] Nanocarriers that can be triggered to release protein cargo in response to changes in temperature, light, pH, redox potential, and enzymatic activities have been reported.[9,20−23] As a result, nanocapsule-mediated delivery of recombinant p53 to cancer cells may be a direct method of reactivating the apoptosis pathway and inducing programmed cell death. One critical limitation of previous protein-containing nanocapsules is that the polymer layer is synthesized from a positively charged monomer that enables nonselective entry across cellular membrane. However, since the level of p53 is tightly

Received: August 6, 2014
Published: October 7, 2014

dx.doi.org/10.1021/ja508083g | J. Am. Chem. Soc. 2014, 136, 15319−15325

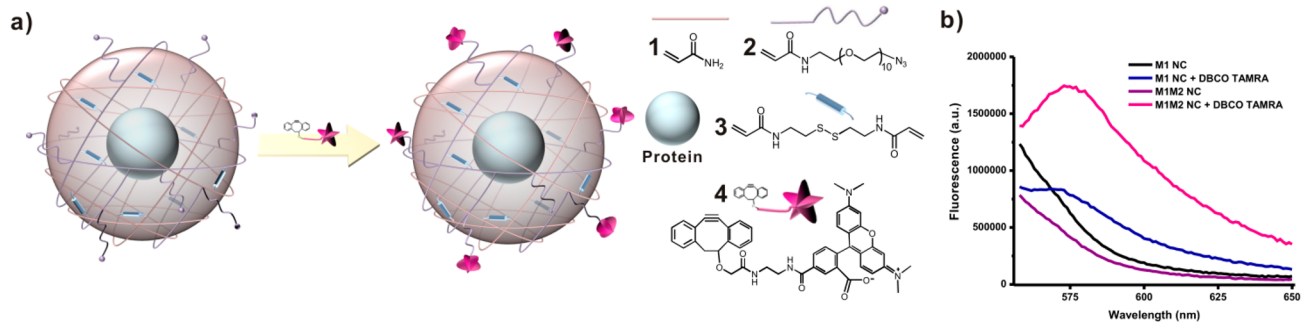

Figure 1. Clickable nanocapsules. (a) Schematic diagram of clickable, redox-sensitive protein nanocapsules and scheme of conjugation to DBCO TAMRA using copper-free click chemistry. (b) Fluorescence spectra of nanocapsule (NC) samples before and after copper-free click conjugation to DBCO TAMRA.

regulated in normal cells, targeted delivery of p53 using functionalized nanocapsules to restrict entry to only cancer cells is highly desirable. Hence, a new nanocapsule encapsulation strategy that allows facile modification of the polymeric carrier is needed.

To equip nanocapsules with cancer-targeting ligands such as peptides and antibodies that can enable receptor-mediated endocytosis, the surface of the nanocapsules must be decorated with reactive handles that facilitate aqueous-based conjugation chemistry. The chemistry utilized must be non-denaturing to maintain the native form of the protein cargo. This is especially important for p53 delivery since the protein forms a tetrameric complex that is prone to aggregation and loss of function.[24] The reaction must also be orthogonal to the nanocapsule synthesis chemistry and compatible with the designed degradation mechanism of the polymer capsule, such as disulfide-mediated redox-sensitive degradation. Among reactions that are compatible with protein-based cargoes, one of the most versatile is the copper-free click chemistry utilizing azides and aryl cyclooctynes.[25−27] Click chemistry has been used to modify nanoparticles for direct conjugation of ligands and chromophores.[28,29] In this report, we demonstrate that PEGylated protein nanocapsules containing reactive azido groups on the surface can be synthesized, allowing facile conjugation to various tumor-targeting ligands. More importantly, we show that recombinant p53 can be selectively delivered to cancer cells using nanocapsules clicked with specific targeting ligands.

RESULTS AND DISCUSSION

Synthesis of Clickable Nanocapsules. Our synthesis strategy for protein nanocapsules is shown in Figure 1. Monomers and redox-sensitive cross-linkers can be deposited at the surface of the protein via van der Waals interactions and can be polymerized in situ around the target protein to form a non-covalent shell that encapsulates the protein. The monomer acrylamide (**1**) is used as a general building block of the water-soluble shell. The nanocapsules are cross-linked with *N*,*N*′-bis(acryloyl)cystamine (**3**), which is designed to degrade in highly reducing environments such as the cytoplasm,[30] thereby releasing the protein cargo intracellularly. To synthesize a near-neutral polymer shell that does not enter cells via positive charges, we first eliminated the use of positively charged monomers employed in previous designs, such as *N*-(3-aminopropyl)methacrylamide. Instead, we chose *N*-azidodeca-(ethylene glycol)ethylacrylamide (**2**) as the second monomer (Figure 1a). Neutral monomer **2** contains a terminal azido group that can be used as the reactive site for cross-coupling via copper-free click reaction. The 10 ethylene glycol units serve as a water-soluble spacer at the surface of the nanocapsules and provide flexibility to the conjugated targeting ligands. Through copolymerization of **1** and **2**, the azido functionalities can be displayed on the surface of the nanocapsules for subsequent modification. Monomer **2** was readily prepared by reacting *O*-(2-aminoethyl)-*O*′-(2-azidoethyl)nona(ethylene glycol) with acryloyl chloride.[29] After purification and mass spectrometric characterization of monomer **2** (Figure S1 in the Supporting Information), we first performed the in situ polymerization process using green fluorescent protein (GFP) as the cargo. Following 1 h of polymerization during which **2** constituted 1.5 mol % of the total monomers, uniformly sized nanocapsules with an electrostatic potential of −0.9 mV and an average size of 9.1 ± 0.8 nm (PDI = 0.32) were synthesized. To examine the structural integrity of the encapsulated proteins, we performed circular dichroism measurements on both free GFP and GFP-containing nanocapsules. As expected, no significant change in the secondary structure of GFP was observed upon encapsulation (Figure S2 in the Supporting Information).

To verify the presence of azido groups on the surface of the nanocapsules, we performed the copper-free reaction between dibenzylcyclooctyne TAMRA (DBCO TAMRA, **4**) and GFP nanocapsules prepared from monomers **1** and **2**. As a control, nanocapsules synthesized from **1** alone were also mixed with **4**. After overnight stirring at 4 °C, the reaction mixture was subjected to repeated dialysis and ultrafiltration [30k molecular weight cutoff (MWCO)] to remove any unreacted **4**. The conjugation of TAMRA to the protein nanocapsules was detected by fluorescence emission scans (Figure 1b). Whereas nanocapsules synthesized with both **1** and **2** exhibited the characteristic TAMRA emission peak at 580 nm, the control sample with only **1** showed nearly no additional signal at the same wavelength compared with negative controls. On the basis of the measured difference between the hydrodynamic radii (R_h) of the GFP nanocapsules (4.5 nm) and free GFP (2.5 nm), we estimate that no more than three GFP can be packed into each nanocapsule. We previously established by experiments that most of the nanocapsules prepared via the interfacial polymerization method contain a single copy of GFP.[31] Taken together, these results indicate that the nanocapsules synthesized here should contain either one or two GFP molecules. The number of TAMRA molecules conjugated per nanocapsule was approximated by comparing of relative intensities of GFP and TAMRA fluorescence. Given the above estimation of one to two GFPs per nanocapsule, we

dx.doi.org/10.1021/ja508083g | J. Am. Chem. Soc. 2014, 136, 15319−15325

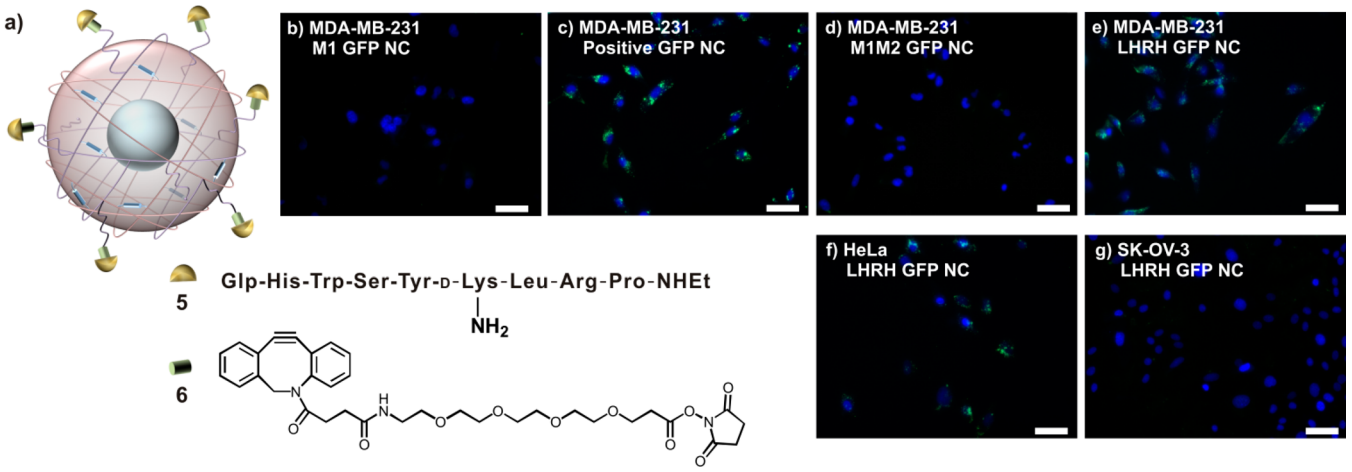

Figure 2. Selective internalization of LHRH-conjugated nanocapsules. (a) Schematic illustration of the LHRH S-S nanocapsule. Glp is cyclized glutamine. (b–g) Fluorescence microscopy images of cell lines treated with 400 nM GFP-containing nanocapsules: (b) MDA-MB-231 cells treated with GFP nanocapsules synthesized with monomer **1** alone; (c) MDA-MB-231 cells treated with positively charged GFP nanocapsules; (d) MDA-MB-231 cells treated with GFP nanocapsules synthesized from monomers **1** and **2** (no targeting ligand); (e) MDA-MB-231 cells treated with GFP nanocapsules synthesized from monomers **1** and **2** and conjugated with the LHRH-targeting ligand; (f) HeLa cells treated with the nanocapsules used in (e); (g) SK-OV-3 cells treated with the nanocapsules used in (e). Nuclei were stained with DAPI (blue). The scale bars represent 50 μm.

approximated that each nanocapsule was conjugated with four to eight TAMRA molecules through the click reaction with accessible azido functional groups.

Conjugation of Nanocapsules with Targeting Ligands. After confirming the successful "clicking" of cyclooctyne moieties onto the surface of azido-functionalized nanocapsules, we then developed methods to conjugate cancer-targeting ligands. We first selected the LHRH peptide Glp-His-Trp-Ser-Tyr-D-Lys-Leu-Arg-Pro-NHEt (**5**) (Figure 2a), which binds to LHRH receptors that are overexpressed in various hormonal related cancers such as breast and prostate cancers.[32] LHRH receptors are not expressed detectably in most visceral organs and have been targeted in the delivery of small molecules.[33,34] Bifunctional dibenzocyclooctyne-PEG4-*N*-hydroxysuccinimidyl ester (DBCO-PEG4-NHS ester, **6**) was chosen as the tether (Figure 2a). Peptide **5** was first conjugated to the NHS terminus of **6** through the internal D-Lys designed to serve as a site for coupling. Adduct **7** was verified by LC–MS and purified to homogeneity by HPLC (Figure S3 in the Supporting Information). Subsequently, **7** was added to the azido-functionalized GFP nanocapsules at a molar ratio of 15:1 and allowed to react overnight at 4 °C. Following the click reaction, unreacted **7** was removed through ultrafiltration (30k MWCO), and the nanocapsules were dialyzed into phosphate-buffered saline. To test the LHRH-receptor-mediated endocytosis of nanocapsules, we added the LHRH-functionalized nanocapsules to MDA-MB-231 cells, which are known to overexpress the receptor.[35] As controls we also added GFP nanocapsules that (i) were positively charged and expected to be internalized [synthesized from monomers **1** and *N*-(3-aminopropyl)methacrylamide]; (ii) were azido-functionalized but not conjugated to LHRH (synthesized from monomers **1** and **2**); and (iii) did not contain azido groups (synthesized from monomer **1** only). After overnight incubation, the internalization of nanocapsules was visualized by fluorescence microscopy (Figure 2b–e).

As can be seen from Figure 2c, the positively charged nanocapsules were well-internalized as expected. In contrast, the neutral nanocapsules, either with or without azido groups, were not internalized into cells at all (Figure 2b,d). LHRH-functionalized GFP nanocapsules, however, were efficiently internalized, as can be seen from the GFP fluorescence in the cytoplasm (Figure 2e). To quantify the extent of internalization through the LHRH receptor, flow cytometry measurements were performed on samples, as shown in Figure 3a. The level of internalization through LHRH-receptor-mediated endocytosis was ~70% of that observed with positively charged nanocapsules. More importantly, azido-functionalized nanocapsules without LHRH conjugation did not exhibit noticeable internalization compared to no treatment or native GFP controls. Trafficking experiments were performed for the LHRH-targeted GFP nanocapsules (Figure 3b,c). Localization in the early endosomes was observed within 30 min, while release into the cytoplasm was detected at 1 and 2 h after delivery. No significant localization of GFP in the late endosome was observed.

To further test the selectivity of the protein delivery, we added the LHRH-functionalized nanocapsules to several cell lines with varying expression levels of LHRH receptor. When LHRH-functionalized nanocapsules were added to cervical cancer cell line (HeLa) cells that have comparable levels of expression, the amount of internalization was similar to that of MDA-MB-231 (Figure 2f). No internalization was seen with the SK-OV-3, which is an LHRH-receptor-negative ovarian cancer cell line (Figure 2g).[36] We then examined the targeting and internalization of the LHRH-targeted GFP nanocapsules after exposing them to Dulbecco's modified Eagle's medium (DMEM) containing fetal bovine serum (FBS) at 37 °C for 24 and 48 h. No attenuation in internalization was observed compared to untreated nanocapsules, suggesting that the targeting mechanism remained intact and the nanocapsules were stable under serum culture conditions (Figure S5 in the Supporting Information).

To demonstrate the versatility of the surface functionalization, we conjugated the single-chain variable fragment (scFv) of the anti-Her2 antibody to the azido-functionalized GFP nanocapsules. A maleimide-containing bifunctional linker was used to react with the cysteine residue on the recombinant scFv at a linker to antibody molar ratio of 5:1 (Figure S6 in the Supporting Information). The extent of conjugation was

dx.doi.org/10.1021/ja508083g | J. Am. Chem. Soc. 2014, 136, 15319–15325

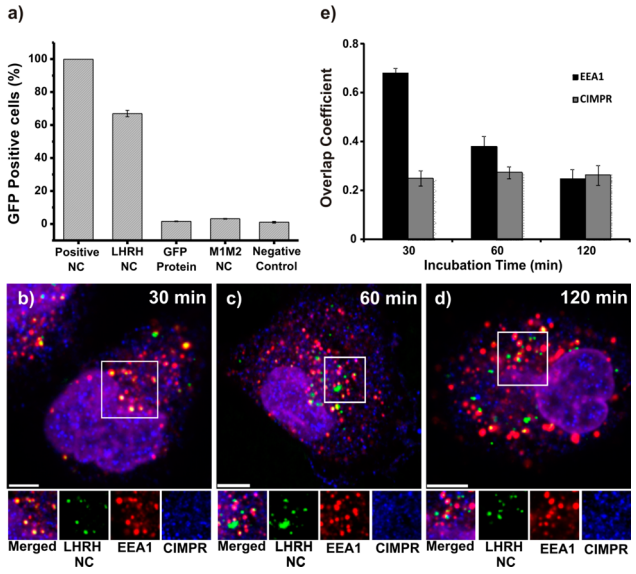

Figure 3. Cellular uptake and trafficking of LHRH nanocapsules by MDA-MB-231 cells. (a) Cellular internalization of 400 nM GFP protein or nanocapsules by MDA-MB-231 cells at 37 °C for 12 h. The mean fluorescence intensity was measured by flow cytometry and is represented as the percentage of fluorescence from MDA-MB-231 cells incubated with positively charged nanocapsules. (b–d) Trafficking of LHRH-conjugated GFP nanocapsules through endosomes. MDA-MB-231 cells were incubated with 800 nM nanocapsules at 37 °C for (a) 30, (b) 60, and (c) 120 min. Early endosomes were detected by early endosome antigen 1 (EEA1) (green). Late endosomes were detected by cation-independent mannose-6-phosphate receptor (CI-MPR) (blue). Nuclei were stained with DAPI and are shown as purple. The scale bar represents 10 μm. (e) Quantification of LHRH-conjugated GFP nanocapsules colocalized with EEA1 or CI-MPR at various incubation time points. Colocalization coefficients were calculated using Manders' overlap coefficient (>10 samples). The error bars indicate standard deviations.

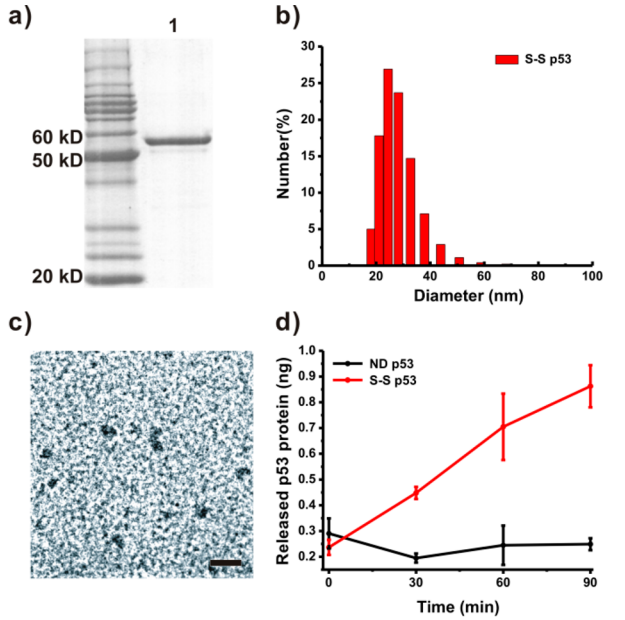

Figure 4. Preparation of recombinant p53 and characterization of LHRH-conjugated p53 nanocapsules. (a) SDS-PAGE of refolded p53 protein. (b) Hydrodynamic size distribution of S-S p53 NCs as measured by DLS. (c) TEM image of S-S p53 NCs. The scale bar represents 50 nm. (d) ELISA assay measuring p53 released from S-S p53 NCs and ND p53 NCs after treatment with 2 mM DTT over 90 min at 37 °C (n = 2).

calculated on the basis of the relative protein concentrations of scFv and GFP in the HER2-conjugated GFP nanocapsules. The total protein concentration of anti-HER2 scFv-conjugated GFP nanocapsules was first determined by the Bradford method, and the concentration of GFP was determined by measuring the fluorescence of the nanocapsules, which was correlated to the GFP concentration using a standard line (Figure S6). The difference between the total protein concentration and the GFP concentration was then attributed to the conjugated anti-HER2 scFv. The ratio of the anti-HER2 scFv and GFP concentrations gives the number of conjugated scFv molecules per GFP-containing nanocapsule. When the scFv to protein nanocapsule molar ratio was kept at 10:1 during reaction, the number of scFv molecules conjugated was estimated to be three to six, assuming either one or two GFPs per nanocapsule, respectively. Upon administration to various cell lines, internalization of GFP was observed only in SK-BR-3 cells, which overexpress the HER2 receptor, and no fluorescence was seen in triple-negative breast cancer cell line MDA-MB-231, HeLa, or human foreskin fibroblasts (HFF) (Figure S6). Collectively, these data illustrate that the polymerization, conjugation, and internalization steps are all effective as designed.

Synthesis of Clickable p53 Nanocapsules. We then applied the nanocapsule synthetic steps toward the targeted delivery of p53 to cancer cells. Delivery of recombinant p53 poses significant challenges, as the tetrameric complex can readily aggregate and lose activity under non-native conditions.[37] The three-dimensional structure of p53 is also not well resolved and has been shown to be loosely organized, especially in the absence of DNA.[24] Recombinant p53 was expressed in *Escherichia coli*, purified from inclusion bodies, and refolded as soluble tetrameric protein (Figure 4a).[37] The in situ polymerization process using monomers **1** and **2** as well as cross-linker **3** was optimized to minimize aggregation and precipitation of the soluble p53. A final **2** content of 1.5 mol % was used in the monomers, while 5 mol % **3** was added as cross-linkers. We found that the p53 concentration had to be kept below 0.7 mg/mL and all of the steps had to be performed in buffer containing sodium bicarbonate to avoid aggregation and precipitation (see the Supporting Information). After encapsulation, the azido-functionalized nanocapsules (S-S p53 NCs) were buffer-exchanged and concentrated in phosphate-buffered saline. Successful encapsulation was monitored by both dynamic light scattering (DLS) (Figure 4b) and transmission electron microscopy (TEM) (Figure 4c). The native p53 tetramer exhibited a hydrodynamic diameter of 7.7 ± 0.5 nm (PDI = 0.27), in line with cryo-EM characterizations.[38,39] Upon encapsulation, the average diameter increased to 27.5 ± 1.0 nm (PDI = 0.39) with a ζ potential of −0.6 mV, and the structural uniformity was observed by TEM. As a nondegradable control, p53-containing nanocapsules cross-linked with *N*,*N*′-methylenebis(acrylamide) were also prepared. The physical properties of the azido-functionalized nondegradable p53 nanocapsules (ND p53 NCs) were nearly identical to those of the S-S p53 NCs.

To examine the encapsulation effectiveness and redox-sensitive release of the p53 nanocapsules, we performed time-dependent enzyme-linked immunosorbent assay (ELISA) analysis of p53 nanocapsules in the presence or absence of the reducing agent dithiothreitol (DTT) (Figure 4d). The

dx.doi.org/10.1021/ja508083g | J. Am. Chem. Soc. 2014, 136, 15319–15325

ELISA assay employed here requires the p53 to bind to a specific double-stranded target oligonucleotide immobilized on strip well plates. Therefore, encapsulated p53 is physically shielded by the polymer layer and is thus unable to bind to the oligonucleotide and to be recognized by the anti-p53 antibody. As expected, in the absence of DTT no native p53 in the solution could be detected within the assay period, indicating the robustness of the polymer layer in both shielding and retaining the p53 cargo. In contrast, the S-S p53 NCs released p53 when 2 mM DTT was added to the nanocapsules, indicating degradation of the cross-linker and release of p53 into the solution. The positive ELISA signal also signifies that the p53 protein subjected to encapsulation and release remained functional. The ND p53 NCs control did not release detectable p53 in the presence of 2 mM DTT, further confirming the redox-responsive nature of the S-S p53 NCs.

Internalization and Release of p53 in Cancer Cells. To examine the internalization of S-S p53 NCs into cancer cells, we first conjugated the recombinant p53 to rhodamine dye to obtain Rho-p53. Following encapsulation with **1**, **2**, and **3** to form rhodamine-labeled NCs, LHRH peptide **5** was conjugated to the surface using bifunctional linker **6**. When the rhodamine-labeled NCs were added to MDA-MB-231 cells, rhodamine fluorescence can be detected within the cells after a 12 h incubation period. In confocal microscopy analysis, we observed the accumulation of Rho-p53 in the nuclei of the targeted cells, which is the expected localization for the transcription factor (Figure 5b). In contrast, no overlap between DAPI and rhodamine fluorescence was observed when Rho-p53 was encapsulated using the nondegradable linker and internalized. This is consistent with the inability of Rho-p53 to escape the polymer shell in the absence of redox-sensitive cross-linker **3**. In this case, all of the rhodamine signals remained in the cytoplasm (Figure 5a).

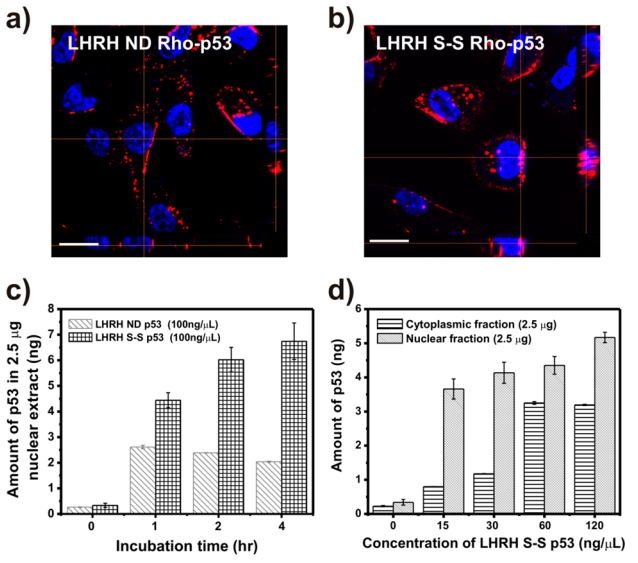

Figure 5. Internalization and location of p53 delivered by designed nanocapsules. (a, b) Confocal images of MDA-MB-231 cells incubated with 200 nM (a) LHRH-conjugated ND Rho-p53 NCs and (b) LHRH-conjugated S-S Rho-p53 NCs. The scale bars represent 20 μm. (c) ELISA detection of p53 in the nuclear fraction from MDA-MB-231 cells treated with 100 ng/μL LHRH-conjugated ND p53 NCs or LHRH-conjugated S-S p53 NCs for increasing periods of time. (d) ELISA detection of p53 in the cytoplasmic and nuclear fraction from MDA-MB-231 cells treated with increasing concentrations of LHRH-conjugated S-S p53 NC for 1 h.

To further quantify the nuclear localization of delivered p53, we performed time-course ELISA analyses of the p53 concentration in both the nuclear and cytoplasmic fractions of MDA-MB-231 cells treated with 100 ng/μL S-S p53 NCs or ND p53 NCs functionalized with LHRH peptide (Figure 5c). The standard curve relating the ELISA signal and the p53 level was established using purified recombinant p53. Untreated cells displayed a low level of endogenous p53 (R280K mutant in MDA-MB-231) that was less than 0.5 ng per 2.5 mg of nuclear extract. As shown in Figure 5c, samples treated with S-S p53 NCs showed a clear accumulation of p53 in the nuclei at the time points tested. Close to 7 ng of p53 per 2.5 mg of nuclear extract was observed after 4 h. As expected from the Rho-p53 localization studies above, significantly higher amounts of p53 were detected in S-S samples compared with nondegradable samples. While the sample treated with ND p53 NCs showed ~2 ng of nuclear p53 after 1 h of treatment, no increase was observed at prolonged incubation times. The effect of the S-S p53 NC dosage on the intracellular p53 concentration was also measured using ELISA. Increasing the amount of LHRH-functionalized S-S p53 NCs (from 15 to 120 ng/L) led to increases in both the cytoplasmic and nuclear concentrations of p53 after 1 h (Figure 5d). Therefore, we have shown that LHRH-functionalized, redox-sensitive nanocapsules can effectively deliver recombinant p53 into cancer cells. The delivered and released p53 can dramatically increase the concentration of p53 in both the cytoplasm and nuclei. The accumulation in the nuclei of cancer cells is especially important, as this is the desired site of action for p53 to reverse the fate of cancer cells.

Cytotoxicity of p53 Nanocapsules. To examine the effect of delivered p53 on cell viability, we performed cytotoxicity studies using the LHRH-functionalized nanocapsules. Two different versions of p53 were used, the wild type and the tumor-selective p53 "supervariant". The super p53 has the gain of the function point mutant S121F, which has been shown to display more potent apoptotic activity.[40] The mutation alters the specificity of p53 in binding its targets, and in particular, attenuates the activation of MDM2 transcription associated with normal p53 overexpression.[40] The decreased MDM2 feedback control therefore increases apoptosis induction. The S121F mutant kills tumor cells irrespective of p53 status but not wild-type mouse embryo fibroblasts.[40] S-S S121F NCs were prepared in the same manner as S-S p53 NCs and conjugated to LHRH peptides using click chemistry. Physical characterizations were performed to verify that the nanocapsules were nearly identical in properties. The two types of LHRH-conjugated nanocapsules were then added to different cancer cell lines, and the cytotoxicities were measured using MTS assay after 48 h. As shown in Figure 6, LHRH-conjugated S-S p53 NCs showed high selectivity toward MDA-MB-231 cells, which overexpress the LHRH receptor. Nearly no toxicity was observed toward either SK-OV-3 or HFF cells at 800 nM, the highest concentration assayed. The S121F-containing nanocapsules showed potent cytotoxicity, with IC_{50} at ~100 nM. In contrast, IC_{50} for the wild-type p53 nanocapsules was ~300 nM. We confirmed that the observed cell death after delivery of S121F was indeed via apoptosis by using the TUNEL assay (Figure S7 in the Supporting Information). Negative controls were used to ensure that the observed toxicity was due to the combination of targeted delivery of p53 and the tumor-selective variant, including (i) azido-functionalized S-S S121F NCs not

dx.doi.org/10.1021/ja508083g | J. Am. Chem. Soc. 2014, 136, 15319−15325

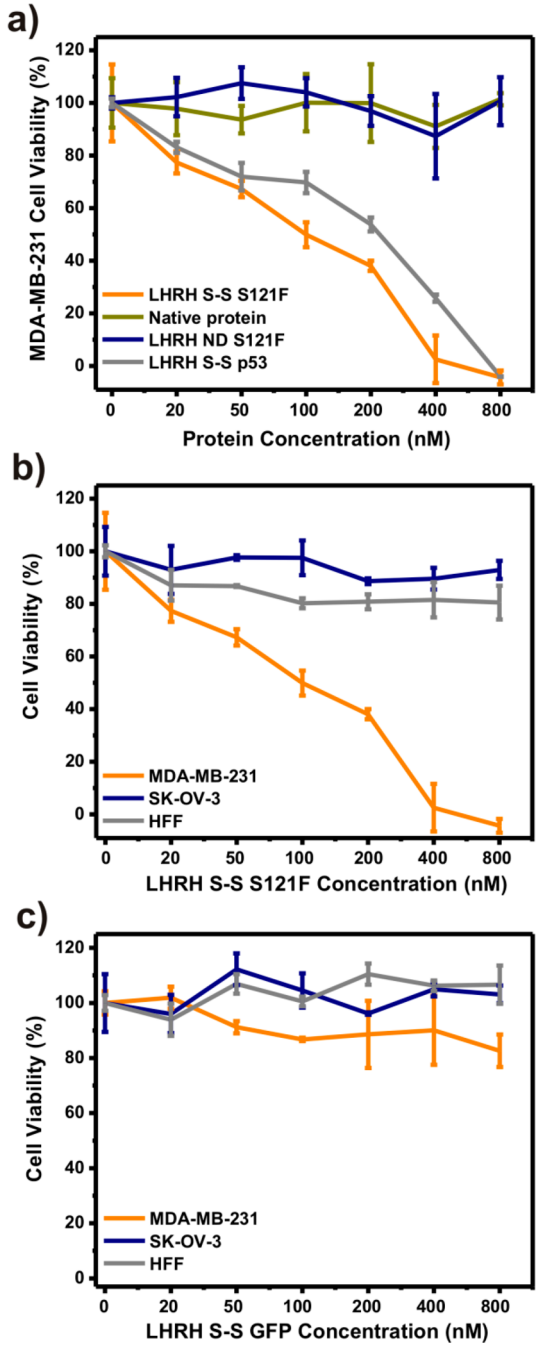

Figure 6. Cytotoxicities of LHRH-conjugated nanocapsules toward cancer cell lines. (a) Viability of MDA-MB-231 cells treated with LHRH-conjugated S-S S121F NCs, native S121F protein, LHRH-conjugated ND S121F NCs, and LHRH-conjugated S-S p53 NCs. (b) Viability of MDA-MB-231, SK-OV-3, and HFF cells treated with LHRH-conjugated S-S S121F NCs. (c) Viability of MDA-MB-231, SK-OV-3 and HFF cells treated with LHRH-conjugated S-S GFP NCs.

conjugated to LHRH, (ii) LHRH-conjugated S−S GFP NCs, and (iii) azido-functionalized GFP NCs not conjugated to LHRH (Figure S8 in the Supporting Information). In all of these controls, the cells remained unaffected by the addition of nanocapsules. These results therefore unequivocally confirm that targeted and functional delivery of p53 can be achieved using the encapsulation and conjugation strategies.

CONCLUSIONS

We developed a new polymerization strategy for the synthesis of protein nanocapsules that display azido functional groups on the surface. By the use of a cyclooctyne and NHS ester- or maleimide-containing bifunctional linkers, different targeting ligands such as the LHRH peptide and anti-HER2 scFv can be attached to the surface of the protein nanocapsules. Using GFP as the cargo, we demonstrated the specific internalization of the nanocapsules into cells overexpressing corresponding receptors. Finally, we demonstrated that this approach can achieve the functional delivery of the genome guardian p53 protein to trigger apoptosis in targeted cancer cells. LHRH-conjugated nanocapsules can be used as a protein delivery system for the treatment of tumor cells overexpressing LHRH receptor. Our results validate a general approach for targeted intracellular protein delivery in a cellular-responsive manner, opening up new opportunities for the development of protein anticancer treatment.

ASSOCIATED CONTENT

Supporting Information

Materials and methods, experimental details, and spectroscopic data. This material is available free of charge via the Internet at http://pubs.acs.org.

AUTHOR INFORMATION

Corresponding Author

yitang@ucla.edu

Notes

The authors declare no competing financial interest.

ACKNOWLEDGMENTS

This work was supported by a David and Lucile Packard Foundation Grant to Y.T. and a CDMRP BCRP Idea Award (BC101380) to Y.T. and P.W.

REFERENCES

(1) Cotter, T. G. *Nat. Rev. Cancer* **2009**, *9*, 501.
(2) Coles, C.; Condie, A.; Chetty, U.; Steel, C. M.; Evans, H. J.; Prosser, J. *Cancer Res.* **1992**, *52*, 5291.
(3) Lacroix, M.; Toillon, R. A.; Leclercq, G. *Endocr.-Relat. Cancer* **2006**, *13*, 293.
(4) Blagosklonny, M. V. *Int. J. Cancer* **2002**, *98*, 161.
(5) Senzer, N.; Nemunaitis, J.; Nemunaitis, M.; Lamont, J.; Gore, M.; Gabra, H.; Eeles, R.; Sodha, N.; Lynch, F. J.; Zumstein, L. A.; Menander, K. B.; Sobol, R. E.; Chada, S. *Mol. Cancer Ther.* **2007**, *6*, 1478.
(6) Issaeva, N.; Bozko, P.; Enge, M.; Protopopova, M.; Verhoef, L. G. G. C.; Masucci, M.; Pramanik, A.; Selivanova, G. *Nat. Med.* **2004**, *10*, 1321.
(7) Vassilev, L. T.; Vu, B. T.; Graves, B.; Carvajal, D.; Podlaski, F.; Filipovic, Z.; Kong, N.; Kammlott, U.; Lukacs, C.; Klein, C.; Fotouhi, N.; Liu, E. A. *Science* **2004**, *303*, 844.
(8) Friedler, A.; Hansson, L. O.; Veprintsev, D. B.; Freund, S. M. V.; Rippin, T. M.; Nikolova, P. V.; Proctor, M. R.; Rudiger, S.; Fersht, A. R. *Proc. Natl. Acad. Sci. U.S.A.* **2002**, *99*, 937.
(9) Lee, Y.; Ishii, T.; Cabral, H.; Kim, H. J.; Seo, J. H.; Nishiyama, N.; Oshima, H.; Osada, K.; Kataoka, K. *Angew. Chem., Int. Ed.* **2009**, *48*, 5309.
(10) Liechty, W. B.; Chen, R. J.; Farzaneh, F.; Tavassoli, M.; Slater, N. K. H. *Adv. Mater.* **2009**, *21*, 3910.
(11) Hu, Y. H.; Atukorale, P. U.; Lu, J. J.; Moon, J. J.; Um, S. H.; Cho, E. C.; Wang, Y.; Chen, J. Z.; Irvine, D. J. *Biomacromolecules* **2009**, *10*, 756.

(12) Giannotti, M. I.; Esteban, O.; Oliva, M.; Garcia-Parajo, M. F.; Sanz, F. *Biomacromolecules* **2011**, *12*, 2524.
(13) Wu, X. J.; Wu, S. Q.; Yang, L.; Han, J. H.; Han, S. F. *J. Mater. Chem.* **2012**, *22*, 17121.
(14) Zheng, C.; Zhang, X. G.; Sun, L.; Zhang, Z. P.; Li, C. X. *J. Mater. Sci.* **2013**, *24*, 931.
(15) Huang, X. L.; Meng, X. W.; Tang, F. Q.; Li, L. L.; Chen, D.; Liu, H. Y.; Zhang, Y. Q.; Ren, J. *Nanotechnology* **2008**, *19*, No. 445101.
(16) Chorny, M.; Hood, E.; Levy, R. J.; Muzykantov, V. R. *J. Controlled Release* **2010**, *146*, 144.
(17) Cho, M. H.; Lee, E. J.; Son, M.; Lee, J. H.; Yoo, D.; Kim, J. W.; Park, S. W.; Shin, J. S.; Cheon, J. *Nat. Mater.* **2012**, *11*, 1038.
(18) Jiang, T.; Mo, R.; Bellotti, A.; Zhou, J.; Gu, Z. *Adv. Funct. Mater.* **2014**, *24*, 2295.
(19) Gu, Z.; Biswas, A.; Zhao, M. X.; Tang, Y. *Chem. Soc. Rev.* **2011**, *40*, 3638.
(20) Zhao, M. X.; Biswas, A.; Hu, B. L.; Joo, K. I.; Wang, P.; Gu, Z.; Tang, Y. *Biomaterials* **2011**, *32*, 5223.
(21) Zhao, M. X.; Hu, B. L.; Gu, Z.; Joo, K. I.; Wang, P.; Tang, Y. *Nano Today* **2013**, *8*, 11.
(22) Murthy, N.; Thng, Y. X.; Schuck, S.; Xu, M. C.; Fréchet, J. M. J. *J. Am. Chem. Soc.* **2002**, *124*, 12398.
(23) Murthy, N.; Xu, M.; Schuck, S.; Kunisawa, J.; Shastri, N.; Fréchet, J. M. J. *Proc. Natl. Acad. Sci. U.S.A.* **2003**, *100*, 4995.
(24) Bell, S.; Klein, C.; Muller, L.; Hansen, S.; Buchner, J. *J. Mol. Biol.* **2002**, *322*, 917.
(25) Mbua, N. E.; Guo, J.; Wolfert, M. A.; Steet, R.; Boons, G. J. *ChemBioChem* **2011**, *12*, 1912.
(26) Ning, X. H.; Guo, J.; Wolfert, M. A.; Boons, G. J. *Angew. Chem., Int. Ed.* **2008**, *47*, 2253.
(27) Baskin, J. M.; Prescher, J. A.; Laughlin, S. T.; Agard, N. J.; Chang, P. V.; Miller, I. A.; Lo, A.; Codelli, J. A.; Bertozzi, C. R. *Proc. Natl. Acad. Sci. U.S.A.* **2007**, *104*, 16793.
(28) Koo, H.; Lee, S.; Na, J. H.; Kim, S. H.; Hahn, S. K.; Choi, K.; Kwon, I. C.; Jeong, S. Y.; Kim, K. *Angew. Chem., Int. Ed.* **2012**, *51*, 11836.
(29) Welser, K.; Perera, M. D. A.; Aylott, J. W.; Chan, W. C. *Chem. Commun.* **2009**, 6601.
(30) Meister, A.; Tate, S. S. *Annu. Rev. Biochem.* **1976**, *45*, 559.
(31) Yan, M.; Du, J.; Gu, Z.; Liang, M.; Hu, Y.; Zhang, W.; Priceman, S.; Wu, L.; Zhou, Z. H.; Liu, Z.; Segura, T.; Tang, Y.; Lu, Y. *Nat. Nanotechnol.* **2010**, *5*, 48.
(32) Nagy, A.; Schally, A. V. *Biol. Reprod.* **2005**, *73*, 851.
(33) Dharap, S. S.; Wang, Y.; Chandna, P.; Khandare, J. J.; Qiu, B.; Gunaseelan, S.; Sinko, P. J.; Stein, S.; Farmanfarmaian, A.; Minko, T. *Proc. Natl. Acad. Sci. U.S.A.* **2005**, *102*, 12962.
(34) Dharap, S. S.; Qiu, B.; Williams, G. C.; Sinko, P.; Stein, S.; Minko, T. *J. Controlled Release* **2003**, *91*, 61.
(35) Harris, N.; Dutlow, C.; Eidne, K.; Dong, K. W.; Roberts, J.; Millar, R. *Cancer Res.* **1991**, *51*, 2577.
(36) Dharap, S. S.; Minko, T. *Pharm. Res.* **2003**, *20*, 889.
(37) Bell, S.; Hansen, S.; Buchner, J. *Biophys. Chem.* **2002**, *96*, 243.
(38) Okorokov, A. L.; Sherman, M. B.; Plisson, C.; Grinkevich, V.; Sigmundsson, K.; Selivanova, G.; Milner, J.; Orlova, E. V. *EMBO J.* **2006**, *25*, 5191.
(39) Tidow, H.; Melero, R.; Mylonas, E.; Freund, S. M. V.; Grossmann, J. G.; Carazo, J. M.; Svergun, D. I.; Valle, M.; Fersht, A. R. *Proc. Natl. Acad. Sci. U.S.A.* **2007**, *104*, 12324.
(40) Saller, E.; Tom, E.; Brunori, M.; Otter, M.; Estreicher, A.; Mack, D. H.; Iggo, R. *EMBO J.* **1999**, *18*, 4424.